Effects of Higher Tire Pressures on Strain in Thin AC Pavements

FREDDY L. ROBERTS and BARRY T. ROSSON

ABSTRACT

Since the oil embargo of 1973 and the attendant increase in fuel prices, pressures to increase truck sizes and weights have intensified. A second factor, which has also been on the increase but which has been given little attention, is tire inflation pressures. Inflation pressures have increased from in the vicinity of 80 psi to a typical value of 120 psi found in Texas tire pressure surveys in 1984. The objective of this paper is to evaluate the effect of this increase in tire pressures on tensile strains in thin asphalt concrete pavements. To determine the stress distribution between the tire and the road surface, the researchers used a finite element computer program developed at Texas Transportation Institute to study the effect of tire parameters on road surface friction forces. This computer program was used to develop the vertical pressure distribution and the horizontal surface shear forces for a free-rolling truck tire inflated to both 75 and 125 psi. A series of computer runs was made using ILLI-PAVE to determine the horizontal tensile strains for asphalt concrete surfaces 1, 1.5, 2, and 4 in. thick over an 8-in. granular base with three different moduli and a subgrade soil that is stress sensitive with an initial modulus of 10 ksi. This series of runs showed that increased truck tire pressures increase tensile strain and attendant fatigue cracking dramatically, that some thin pavement structures cannot provide adequate service, and that design procedures must be upgraded to consider pavement materials that can resist these high tensile strains. In general, to provide adequate service, materials should be either thin and flexible or thick and stiff.

During the last few years, pressure on legislatures has concentrated on either increasing gross vehicle weights from current levels to more than 100,000 lb or increasing the size of trailers, or both. Concern over the effects of these increases on pavement deterioration has been so great that highway engineers have largely ignored in their analyses another factor that has also been on the increase: tire inflation pressures. With the increased cost for fuel and the desire to reduce rolling resistance and increase fuel economies, tire manufacturers have responded by designing and marketing both bias and radial tires that operate at higher inflation pressures. This means that pavements that were designed for 70,000- to 80,000-lb gross vehicle weight (GVW) vehicles carrying loads on tires inflated to 75 to 80 psi are now carrying heavier loads at significantly increased tire pressures. To determine the current levels of tire pressures and their effects on Texas highways the Texas State Department of Highways and Public Transportation (SDHPT) contracted with the Texas Transportation Institute (TTI) to perform two research projects. The first project is to determine typical tire inflation pressures, their contact pressure distributions, and their effects on highway pavements. The second project includes evaluation and design of thin asphalt concrete (AC) pavements including evaluation of suitable materials with which to build these thin pavements. This paper includes portions of both of these studies.

TIRE MODELS IN PAVEMENT ANALYSIS

Initial analyses of the states of stress in solid bodies involved the use of point load on uniform elastic materials of semi-infinite extent; later analysis techniques included strip loads of finite width and infinite length. As analysis of pavement systems became more sophisticated, Westergaard and Burmister extended the analysis to include more than one layer and also began to model the tire as a circle of uniform vertical pressure with no surface shear forces. This tire model continued to be used in the highway design community until the last few years. More recently highway engineers have begun to use finite element models developed by tire carcass designers to define the stress conditions that occur at the tire-pavement interface.

Tielking Tire Model

The finite element tire model used in this study was originally developed during an analytical and experimental investigation of tire-pavement interaction (1) to provide the capability for calculating the distributions of sliding velocity and normal pressure in the tire-pavement contact interface. A relatively general, nonlinear finite element shell-of-revolution computer program (2,3) was chosen as the foundation for the finite element tire model. A Fourier transform procedure for solving the shell contact problems of the foundation program was developed (4) and incorporated into the finite element program, giving this tire model the unique capability of calculating contact boundary and interface pressure distribution for a specified tire deflection.

The shell elements used in the tire model are orthotropic. A material property subroutine was developed to generate orthotropic moduli from cord and rubber property data and geometric data describing the ply structure of the tire carcass. Although the shell elements are homogeneous and orthotropic, they are sensitive to details of carcass design including tire materials and geometry.

The tire is modeled by an assemblage of axisymmetric curved shell elements. The elements are connected to form a meridian of arbitrary curvature and are located at the carcass midsurface. Figure 1 shows the assembly of 21 elements along the midsurface of a G78-14 tire. A cylindrical coordinate system is used, with r, w, and z indicating radial, circumferential, and axial directions, respectively. Each element forms a complete ring that is initially axisymmetric with respect to z. The elements are connected at nodal circles (numbered in Figure 1) hereafter referred to as nodes.

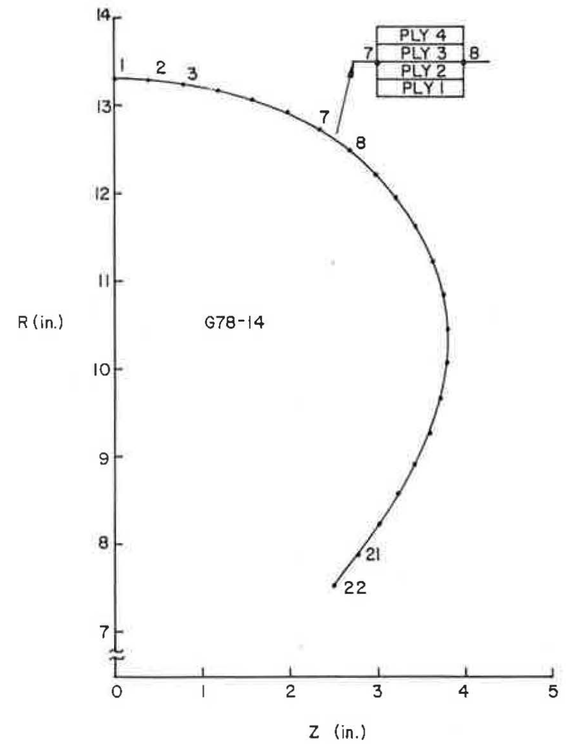

FIGURE 1 Finite elements positioned on the tire carcass midsurface.

The finite elements are homogeneous and orthotropic with a set of moduli specified for each individual element. The orthotropic moduli for each element are determined by the ply structure surrounding the element.

The finite element model is clamped at the edges (Node 22 in Figure 1), pressurized, and rotated to induce centrifugal force loading. It is then brought into contact with a rigid, frictionless surface perpendicular to the plane of symmetry (the r-θ plane). The contact surface (the pavement) is at the specified loaded radius (Rℓ) measured from the z-axis. The internal pressure, the angular velocity, and the loaded radius are the only operating variables specified before contact deformation and pressure in the contact region are calculated. Tielking and Schapery (4) describe the mathematical procedures used to calculate the contact pressure distribution and deformation of the tire deflected against the pavement.

The deflected shape of a nylon tire meridian passing through the center of the contact region is plotted in Figure 2 for tire deflection δ = 0.9 in. Figure 2 also shows both the inflated, undeflected meridian and the calculated contact pressure distribution along the meridian. The calculated tire load is 850 lb (for δ = 0.9 in.).

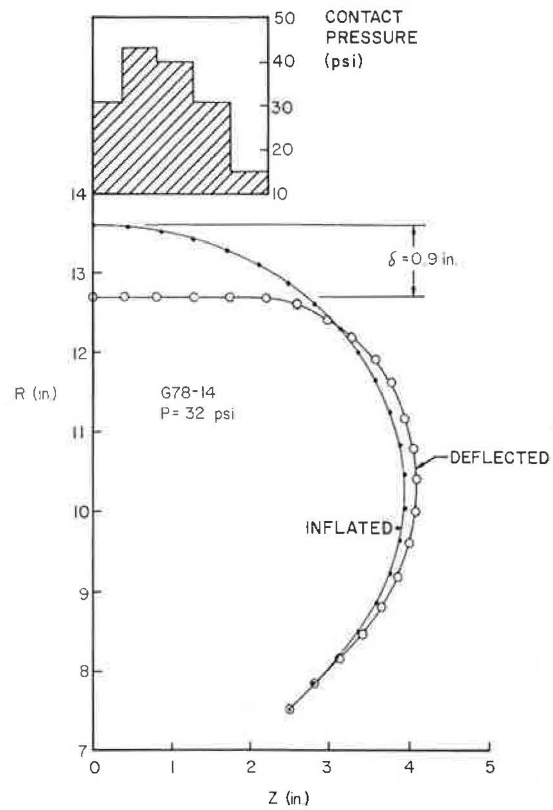

FIGURE 2 Deflected shape and tire contact pressure distribution results from finite element tire model.

This finite element tire model is believed to be the first to have the capability of calculating the contact pressure distribution in the footprint of a deflected tire. This capability is important because contact pressure has a profound influence on all aspects of tire performance. The finite element tire model enables analytical investigations to be made of how tire design variables influence contact pressure distribution.

The rolling-tire results are calculated by superimposing the angular velocity of the rolling tire on the solution for static contact against a frictionless surface. The sliding velocities of points in the contact region are calculated as outlined elsewhere (5). The sliding velocity and the normal contact pressure determine the friction coefficient at each point in the footprint. The resultant braking and driving and steering shear forces respond to tire operating variables such as inflation pressure, tire load, and slip angle through the influence of these operating variables on the distribution of sliding velocity in the footprint. Tire side force is similarly obtained by summing the lateral shear forces in the contact region.

Tire Selected for Study

For the study reported in this paper, a typical 10.00-20 bias-ply truck tire carcass was obtained; the input data were developed by performing measurements on a section of the tire; and the tire pressure distributions were calculated. Figure 3 shows the

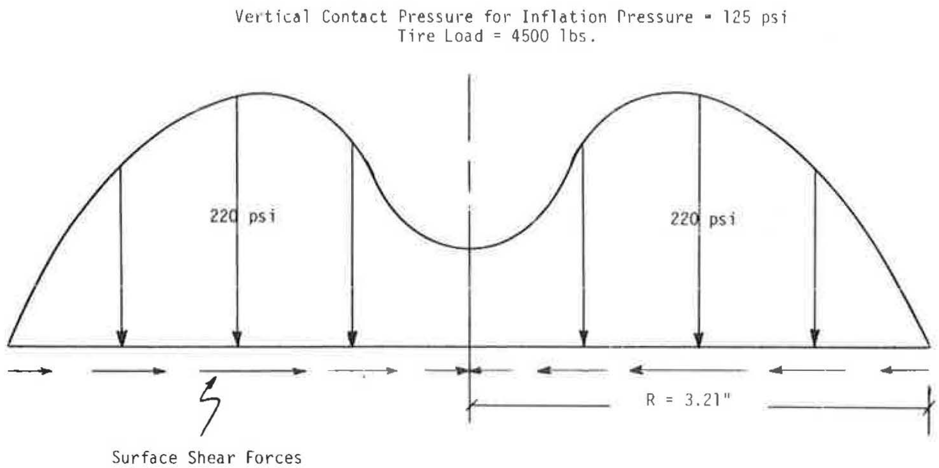

FIGURE 3 Nonlinear vertical tire pressure distribution with lateral surface shear forces as developed using finite element model by Tielking.

vertical and horizontal contact pressure distributions for this tire inflated to 125 psi.

Two tire pressures were selected for this analysis, 75 and 125 psi. These two values were selected because the first value represents a typical historical value used for design and analysis of highway pavement structures, and the second value represents current inflation pressure on Texas highways as shown by a field study conducted by TTI during the spring and summer of 1984. Although the second value may appear high to some readers, representatives from tire manufacturers indicate that within the next 5 years inflation pressures will continue to rise to nearly 150 psi. The impetus for these higher values is reduced rolling resistance, which produces reduced vehicle operating costs.

PAVEMENT MODEL SELECTED FOR ANALYSIS

The computer program used for this analysis is a modified version of ILLI-PAVE (6). This program was chosen over two other programs, PLANE and CRANLAY, because the modified version of ILLI-PAVE had more flexible material property inputs and because tire pressure distribution could be input in a variety of ways.

The computer programs PLANE and CRANLAY were written by Harrison, Wardle, and Gerrard in Australia in 1972 (7). PLANE is an elastic layer theory program that only considers a single layer of infinite depth with material property inputs defined elastically in two directions as orthorombic, cross-anisotropic, or isotropic. The tire load is represented as a strip of specified width and magnitude but infinite in extent. There are, however, 12 different load cases that can occur in pairs: uniform and linear vertical stress, uniform and linear lateral shear stress, and displacement-defined loads.

CRANLAY is also an elastic layer theory program with the capability of accepting up to five horizontal layers with material properties defined as either cross-anisotropic or isotropic. Tire load is input as a circular load of specified radius and magnitude. CRANLAY has only two different load cases, which must be run separately: uniform vertical pressure and linear radial shear stress. Both programs output the stresses, strains, and displacements in the layer or layers of the system.

The third pavement program examined was ILLI-PAVE. It is a version of a program written by Wilson (8-10) that was modified and made user friendly by the research staff of the Construction Engineering Laboratory at Champaign, Illinois, in 1982. It is a finite element program that models a pavement three dimensionally by using a two-dimensional half space of a finite solid of revolution. This rectangular half space is divided into a set of rectangular elements connected at their nodal points. ILLI-PAVE loading is of the "flexible plate" type (i.e., a uniform circular contact pressure). The material modular properties of ILLI-PAVE can be input as a function of the minor principal stress, the deviator stress, the first stress invariant, or simply as a constant elastic modulus.

This program was selected because it had the material property inputs that were needed and the tire load input capabilities could be changed to allow nonuniform vertical pressure and lateral shear pressures. This was accomplished by externally calculating the UZ and UR load values and reading them directly into the program as input. The uniform contact pressure of the original ILLI-PAVE was set to approximately zero, and the UZ and UR values were read in as the load input. UZ is the variable used to define the vertical force or displacement at a node on the surface, and UR is the variable used to define the horizontal force or displacement at a node. Because the UZ and UR values are generated externally, any desired distribution of load in the vertical or horizontal direction can be input. The UZ and UR values were calculated using the pressure distribution output from the Tielking tire model.

The ILLI-PAVE output gives the displacements of nodes and stresses at the midpoint of the element. Strains in the surface were calculated externally using Hooke's law.

STUDY PARAMETERS

The basic objective of this paper is to evaluate the effects of increased tire pressure on thin asphalt concrete pavements that are typically used on the Texas farm-to-market system. Therefore the following series of material combinations and layer thicknesses was used to determine the stress and strain state for two different tire inflation pressures and a 4,500-lb single wheel load:

- Surface
  Thickness: 1, 1.5, 2, and 4 in. and

Elastic moduli: 50, 100, 200, 400, and 800 ksi.

- Base
  Thickness: 8 in. and
  Elastic moduli: stress-sensitive.

Equation	Typical Base Modulus (psi)
$4886\theta^{0.239}$	20,000
$7000\theta^{0.325}$	40,000
$8787\theta^{0.365}$	60,000

where θ = bulk stress

- Subgrade
  Thickness: infinite and
  Elastic moduli: as defined in Figure 4.
  Note: Only one subgrade soil was included in this analysis.

The tire pressure distributions for most computer runs were based on results from the model developed by Tielking; however, several runs were made using the uniform vertical pressure case. The primary differences that occurred as a result of using these two models are that the inflation pressure and contact pressure are equal for the uniform vertical case and that, when the Tielking model is used, the contact pressure distribution is nonuniform and not equal to the tire inflation pressure. Therefore the tire contact radius for these two pressure cases is different; the uniform pressure case is larger.

STUDY RESULTS

Several types of comparisons will be made using results from the ILLI-PAVE computer runs. These comparisons will include plots to show the effects of tire pressure on horizontal tensile strain at the bottom of the surface, the effects of base modulus on tensile strain, and the effects of both surface thickness and modulus on strains. An additional analysis is included to evaluate the effect of tensile strains on predicted fatigue damage through the use of a fatigue damage factor. Each analysis will be presented separately in the following sections.

Tire Pressure Effects

The series of computer runs used in this analysis is the same set described in the Study Parameters section. All runs for this analysis included a 4,500-lb load with nonuniform vertical pressure and with lateral surface shear forces. To describe the effects of tire pressure on tensile strain, Figures 5 and 6 have been prepared. Figure 5 shows the change in tensile strain for a surface of varying thickness and with a modulus of 400 ksi, and Figure 6 shows the same information for a surface with a modulus of 50 ksi.

The increase in tire pressures produces increases in the strain ranging from 20 to 30 percent for the 1-in. surface data in Figure 5 with the 30 percent increase occurring for the stiffest base layer. Notice that the effect of increased tire pressure decreases with increasing surface thickness and that the relative increase for a 4-in. surface is less than 10 percent.

Figure 6 shows that at 75-psi inflation pressure a surface 1 in. thick is in compression for the moderate and strong bases and that the tensile strain is low for the weak base. However, when the tire pressure increases to 125 psi, the 1-in. surface still remains in compression for the moderate and strong bases but the tensile strain increases dramatically for the weak base condition. For the low

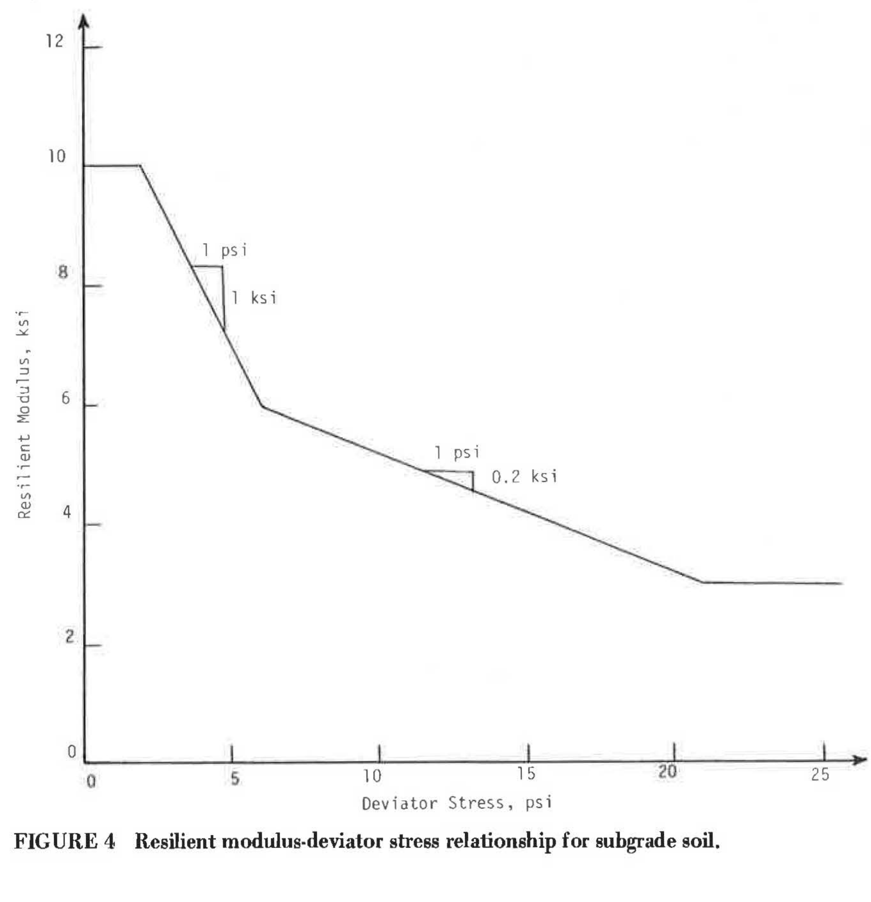

FIGURE 4 Resilient modulus-deviator stress relationship for subgrade soil.

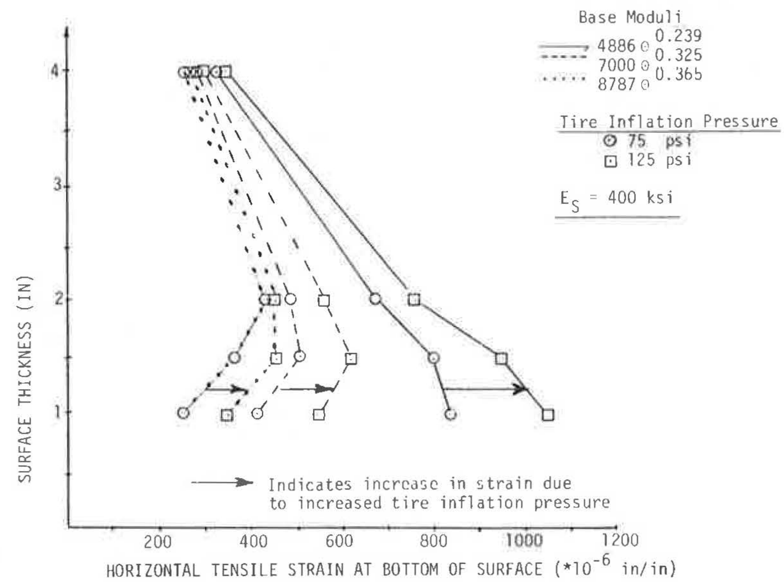

FIGURE 5 Effects of increased tire pressure on tensile strain for a surface modulus of 400 ksi.

modulus base all the thicknesses experience strains near or in excess of 0.001 in. per inch, which Monismith says is the upper limit of linear behavior of these materials: "For strains exceeding 0.001 in./in., asphalt concrete mixtures are nonlinear, rate dependent materials with different properties in tension and compression" (11).

The increases in strain for the 2-in. surface range from about 30 to 55 percent for the weak to strong bases, indicating the significance of the effect of increasing tire pressures on surfaces with low moduli. Therefore it is important to recognize that the general advice often given, to make thin pavements flexible, must be conditioned by adding that the surface thickness should be limited to less than 1.5 in. for moderate and strong bases. Extremely flexible asphalt concrete materials should probably not be used in combination with weak granular bases, especially because tire pressures have increased substantially during the last few years.

For thick flexible surfaces, the increase in tire pressure produces a smaller increase in tensile strain than for thinner surfaces, but the increase in strain for the more flexible surfaces, shown in Figure 6, is much larger than that experienced by the stiffer surfaces shown in Figure 5. In general, as the surface thickness increases, the surface modulus is more important in determining the strain level than the base modulus; however, as the surface thickness decreases, the effect of the base modulus becomes more significant.

Base Modulus Effects

The effects of base modulus are shown more clearly in Figures 7 and 8, which contain plots of strain

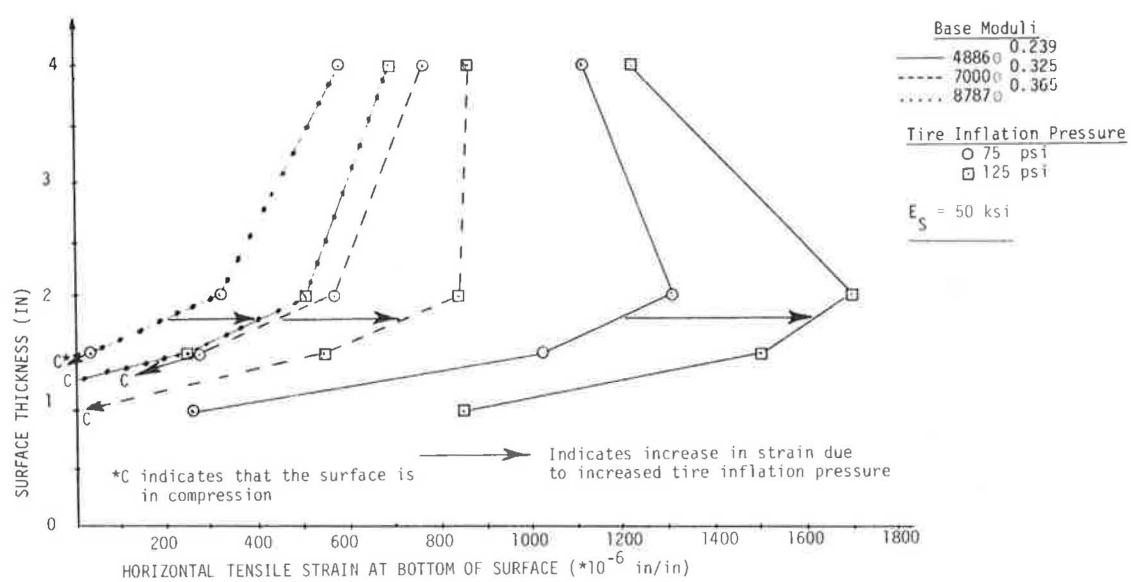

FIGURE 6 Effects of increased tire pressure on tensile strain for a surface modulus of 50 ksi.

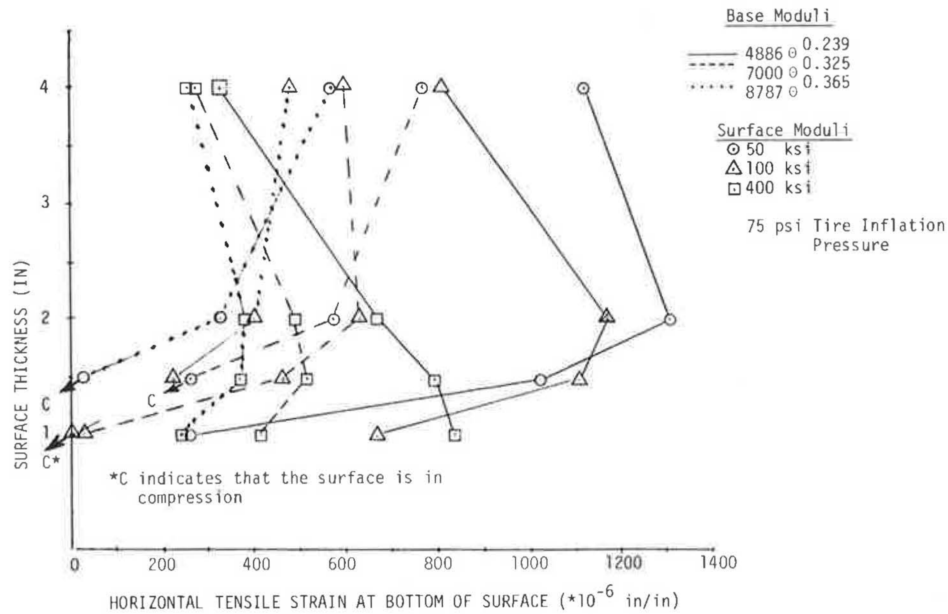

FIGURE 7 Effects of surface and base moduli on tensile strain at the bottom of the surface layer for surface moduli of 50, 100, and 400 ksi and a tire pressure of 75 psi.

for four different surface moduli for each of three different base moduli included in the study. In reviewing the plots of Figures 7 and 8, it is evident that for the stiff and moderate base moduli the 1-in.-thick 50- and 100-ksi modulus surfaces are either in compression or have tensile strains of less than 50 microinches per inch. At these strain levels those material combinations should perform quite adequately in the field. Even for the low base modulus and 50-ksi surface modulus the tensile strain in the 1-in. surface is low enough for quite satisfactory field service. It should be noted that as the tensile strain increases to levels of about 300 microinches per inch, the fatigue life can be expected to be reduced quite significantly.

The plots in Figure 8 show the interaction among base modulus, surface modulus, and surface thickness. For the 4-in. surface the strain is affected more by surface modulus than by base modulus: for the 400- and 800-ksi surfaces the strain values for the three base conditions are clustered together, but for the 50-ksi surface the strains for the different base moduli vary significantly but are still widely separated from the other two sets of surface modulus data. Note that at the 2-in. thickness the data for the three surface moduli began to overlap with the 50-ksi surface modulus covering almost the whole range of the 2-in. data whereas for the other surface moduli the different base stiffnesses begin to cause the strain levels to spread out and to overlap.

At the 1-in. thickness the effect of surface

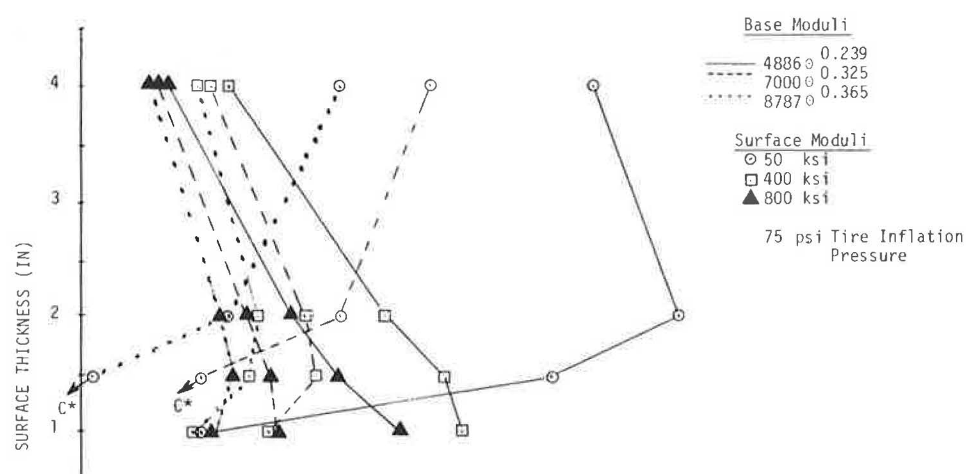

FIGURE 8 Effects of surface and base moduli on tensile strain at the bottom of the surface layer for 50, 400, and 800 ksi surface moduli and a tire pressure of 75 psi.

modulus is slight compared to the effect of the base modulus. Notice that in Figure 8 the points for the 400- and 800-ksi surfaces for each of the base moduli are nearly on top of each other for the high and moderate base moduli are quite close to each other for the low base moduli. At the 1-in. surface thickness the 50-ksi surface is either in compression or the strain level is at a quite acceptable level for adequate performance for low-volume roadways.

The data for 50-ksi and 100-ksi surface moduli in Figures 7 and 8 show that the base modulus effect is greatest for the 2-in. surface thickness. For the 400- and 800-ksi surface moduli the base modulus effect is greatest for the 1-in. surface thickness. For the range of surface thicknesses between 1 and 2 in., there is considerable overlap of the strain at the various combinations of surface and base moduli, and these data indicate the sensitivity of tensile strain to different combinations of thickness, surface modulus, and base modulus.

Surface Modulus and Thickness Effects

To evaluate the effects of surface modulus on strains for different base moduli and tire pressures, Figures 9-11 have been prepared. Each figure contains plots of tensile strain (microinches per inch) at the bottom of the surface for each combination of surface thickness and surface modulus. The plot on the top of each figure is the strain for a 75-psi inflation pressure, and on the bottom is strain for a 125-psi inflation pressure. The contour lines on each figure represent lines of equal strain.

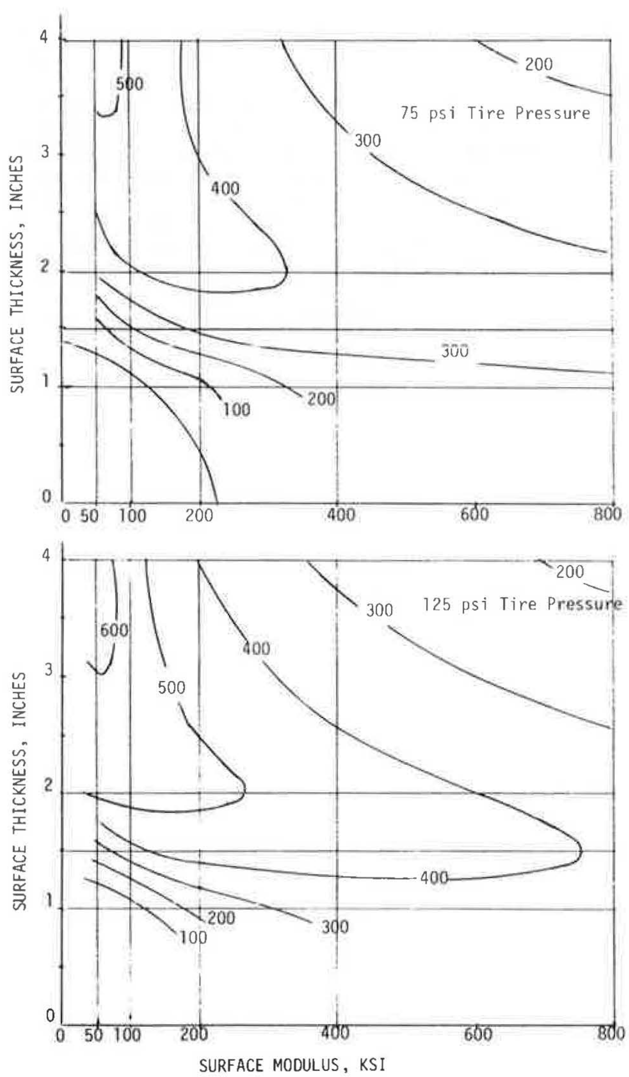

FIGURE 9 Tensile strain contours for $8787\theta^{0.365}$ base modulus.

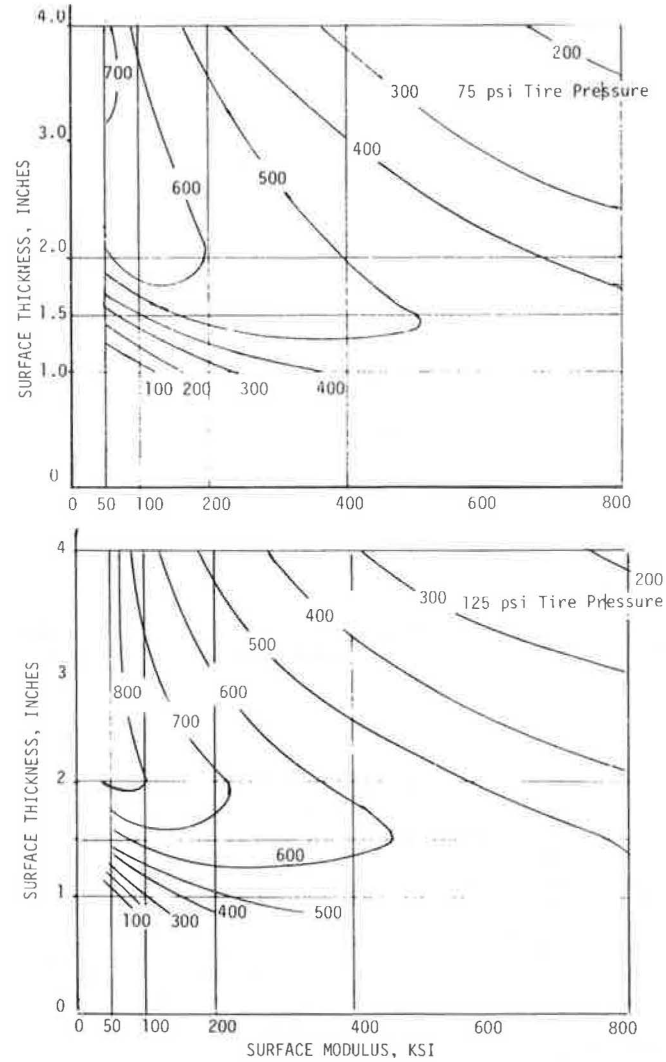

FIGURE 10 Tensile strain contours for $7000\theta^{0.325}$ base modulus.

To resist fatigue damage, the tensile strains in the pavement structure must be kept fairly low, the exact level depending on the total traffic to be carried on the roadway and the characteristics of the surfacing layer. Because low strains are desirable, the first analysis of the plots in Figures 9-11 involved identifying the low strain areas. For purposes of discussion the authors have selected a strain level of 300 microinches per inch as a level below which reasonably adequate performance can be achieved and above which performance begins to be significantly impaired.

Strain levels below 300 occur in both the upper right and the lower left corners in Figures 9 and 10, but only in the upper right corner in Figure 11. Notice also that increasing tire pressure from 75 to 125 psi results in higher strain levels being wedged between the areas of low strain level thereby compressing and driving these low strain levels more toward opposite corners. Increased tire pressure for the weak base condition (Figure 11) resulted in there

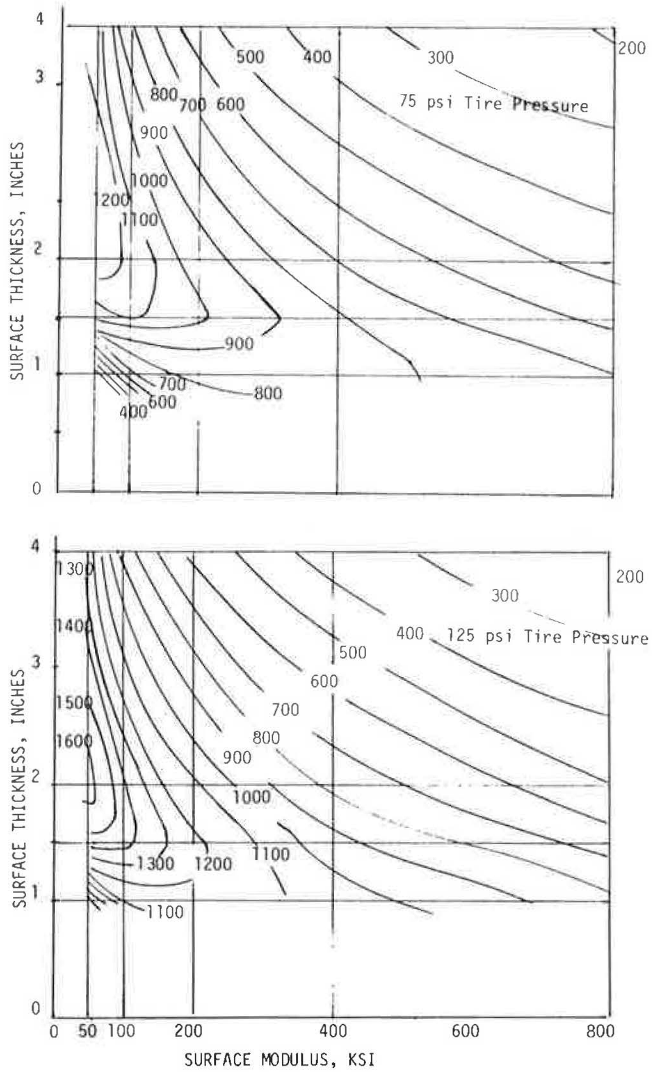

FIGURE 11 Tensile strain contours for $4886\theta^{0.239}$ base modulus.

being no strain level below 300 for the low-modulus surface combinations in the bottom left corner.

Review of the isostrain lines in Figures 9-11 led the authors to conclude that for thin asphalt concrete surfaces the surface moduli should be low and the base moduli for the flexible bases should be high. Only with this combination of materials can tensile strains be reduced to levels that will provide adequate fatigue resistance.

The strain levels for surface thickness of 1.5 to 2 in. are quite high except for the high base modulus combined with surface moduli of more than 300 ksi. At these strain levels reduced service life will occur but pavements with several years of life should result, depending on the traffic levels. For the moderate and weak bases, these high tire pressures produce strains too high to provide even marginal lengths of service life.

To provide a more definite indication of the effects of the interaction between tire pressure and surface thickness and moduli on fatigue cracking, an analysis was conducted to estimate the additional fatigue damage produced by the increase in tire pressure from 75 to 125 psi. To perform this analysis, a fatigue equation developed from AASHO Road Test results was selected (12). The equation was developed by using the observed number of weighted 18-kip equivalent single axle loads (ESALs) required to produce Class 2 fatigue cracking, and the calculated tensile strain at the bottom of the surface layer was developed using ELSYM5. A regression analysis produced the following equation (12):

$$W_{18} = 9.7255 \times 10^{-15} \, (1/\varepsilon)^{5.16267}$$

where

W_{18} = number of weighted 18-kip axle loads before Class 2 cracking and

ε = transverse strain calculated using ELSYM5 for 27 AASHO test sections;

R^2 = 0.9294.

To evaluate the additional damage produced by the increase in tire pressure from 75 to 125 psi, a fatigue damage factor was calculated. The fatigue damage factor is a ratio of the number of 18-kip ESALs that the pavement could sustain at the lower tire pressure divided by the number that could be carried at the higher tire pressure; that is,

$$FDF = (\varepsilon_{p2}/\varepsilon_{p1})^{5.16267}$$

where

FDF = fatigue damage factor,

ε_{p1} = strain at bottom of surface at tire pressure p1 = 75 psi, and

ε_{p2} = strain at bottom of surface at tire pressure p2 = 125 psi.

These fatigue damage factors have been plotted for each combination of surface modulus and thickness and for each base modulus in Figures 12-14. In studying these plots it must be remembered that these factors are relative and not absolute. For example, the fatigue damage factors for surface moduli of 400 and 800 psi in all three figures are quite similar. It could be erroneously concluded that to minimize the effect of increased tire pressure, stiffer pavement structures should be built. That this conclusion is erroneous can be confirmed by looking at Figures 10 and 11 that show that for 1- and 1.5-in.-thick surfaces, the tensile strains are greater than 500 microinches per inch, which is too high for adequate fatigue life.

These plots indicate the significance of the interaction between surface modulus and thickness and its effect on fatigue damage and indicate again that thinner pavements should be as flexible as possible in order to be in compression and thereby bypass the problem of fatigue cracking. Notice that the 1-in.-thick surface with 50- and 100-ksi moduli in Figure 12 is in compression. The data point out the relative sensitivity of thin, lower modulus surface materials to the effects of increased tire pressure and the relative insensitivity of thick, higher modulus materials to increased tire pressure.

CONCLUSIONS

On the basis of the limited results included in this paper, the following tentative conclusions can be drawn:

1. The granular base modulus significantly affects the tensile strains experienced by thin asphalt concrete pavements with the greatest effect at low thicknesses.
2. The surface modulus significantly affects the

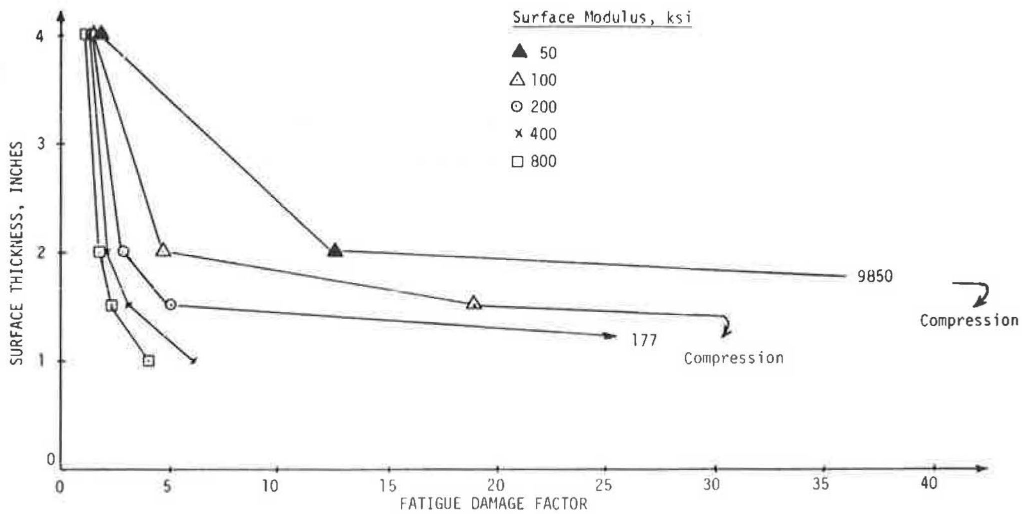

FIGURE 12 Fatigue damage factor due to increasing tire pressure from 75 to 125 psi 8787$\theta^{0.365}$ base modulus.

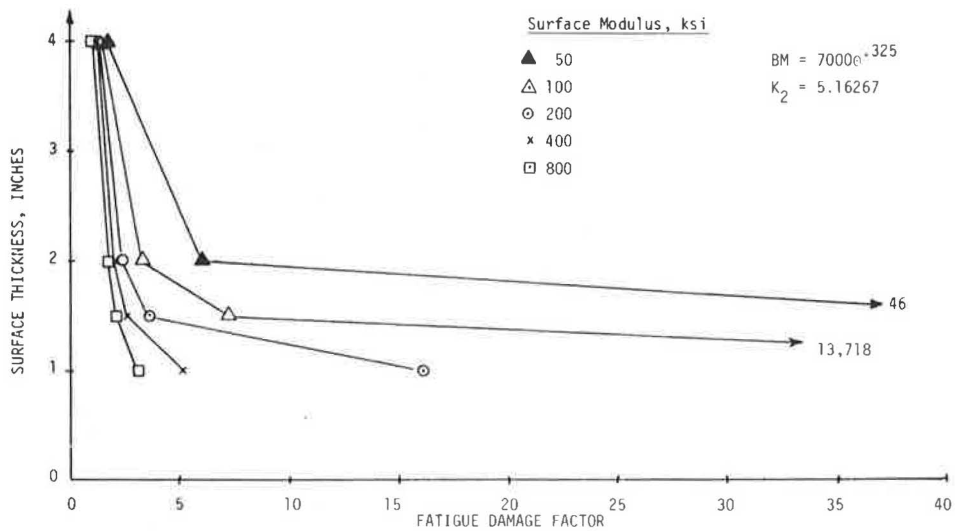

FIGURE 13 Fatigue damage factor due to increasing tire pressure from 75 to 125 psi for 7000$\theta^{0.325}$ base modulus.

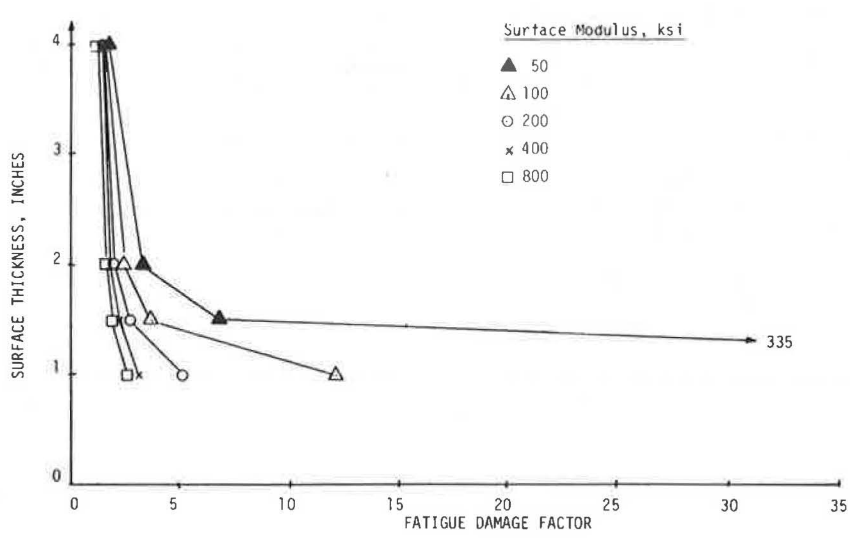

FIGURE 14 Fatigue damage factor due to increasing tire pressure from 75 to 125 psi for 4886$\theta^{0.239}$ base modulus.

tensile strain at the bottom of the surface for thin asphalt layers. A low surface modulus over strong and moderate bases produced compression in the surface, but as the surface modulus increased so did tensile strains.

3. The effect of increased tire pressure on strain was so great for the weak base modulus that normal hot-mixed materials appear to be unsuitable. Only thick layers of extremely stiff surfacing produced low enough strains for satisfactory fatigue lives. The fatigue damage factors, calculated to show the relative effect of increasing tire pressure from 75 to 125 psi, show that the greatest relative effect occurs for low-modulus, thin surfaces.

4. The design of thin pavement structures must include careful consideration of the interactions of base modulus, surface thickness, and surface modulus and their effect on tensile strains. This is especially true if the predominant failure mode for these pavements is fatigue cracking.

ACKNOWLEDGMENTS

The research described in this paper was carried out at the Texas Transportation Institute at Texas A&M University. The authors are grateful for the support of the Texas State Department of Highways and Public Transportation and that of the Federal Highway Administration, U.S. Department of Transportation.

REFERENCES

1. R.A. Schapery and J.T. Tielking. Investigation of Tire-Pavement Interaction During Maneuvering: Theory and Results. Report FHWA-RD-78-72. FHWA, U.S. Department of Transportation, June 1977.
2. J.R. Tillerson and W.E. Haisler. SAMMSOR II--A Finite Element Program to Determine Stiffness and Mass Matrices of Shells of Revolution. TEES-RPT-70-18. Texas A&M University, College Station, Oct. 1970.
3. W.E. Haisler and J.A. Stricklin. SNASOR II--A Finite Element Program for the Static Nonlinear Analysis of Shells of Revolution. TEES-RPT-70-20. Texas A&M University, College Station, Oct. 1970.
4. J.T. Tielking and R.A. Schapery. A Method for Shell Contact Analysis. Computer Methods in Applied Mechanics and Engineering, Vol. 26, No. 2, May 1981, pp. 181-195.
5. J.T. Tielking and R.A. Schapery. Calculation of Tire-Pavement Shear Forces. ASME Symposium Proc., ASME Symposium on The General Problem of Rolling Contact, Vol. 40, 1980, pp. 19-39.
6. ILLI-PAVE--A Finite Element Program for the Analysis of Pavements. Construction Engineering Laboratory and the Transportation Facilities Group, Department of Civil Engineering, University of Illinois at Urbana, May 1982.
7. W.J. Harrison, L.J. Wardle, and C.M. Gerrard. CRANLAY and PLANE--Computer Programs for Circle and Strip Loads on Layered Anisotropic Media. Commonwealth Scientific and Industrial Research Organization, Canberra, Australia 1972.
8. E.L. Wilson. A Digital Computer Program for the Finite Element Analysis of Solids with Non-Linear Material Properties. University of California, Berkeley, 1965.
9. E.L. Wilson. A Digital Computer Program--A Finite Element Analysis of Axisymmetric Solids with Orthotropic, Nonlinear Material Properties. University of California, Berkeley, July 1967.
10. J.M. Duncan, C.L. Monismith, and E.L. Wilson. Finite Element Analysis of Pavements. In Highway Research Record 228, HRB, National Research Council, Washington, D.C., 1968, pp. 18-33.
11. C.L. Monismith. Fatigue Characteristics of Asphalt Paving Mixtures and Their Use in Pavement Design. Symposium on Fatigue in Asphalt Pavements, Albuquerque, University of New Mexico, Jan. 7, 1981.
12. Asphalt Concrete Overlays of Flexible Pavements, Vol. 1: Development of New Design Criteria. Report FHWA-RD-75-75. FHWA, U.S. Department of Transportation, June 1975.

Publication of this paper sponsored by Committee on Flexible Pavements.